



## Characterization of Synthesized Goethite and Natural Goethite sourced from Itakpe in North Central, Nigeria

Abdus-Salam N.<sup>1</sup>, \*Ugbe F.A.<sup>2</sup> and Funtua M.A.<sup>3</sup>

<sup>1</sup>Department of Chemistry, Faculty of Physical Sciences, University of Ilorin, Ilorin, Nigeria.

<sup>2</sup>HQ 1 Division Supply and Transport Nigerian Army, Kaduna, Nigeria.

<sup>3</sup>Department of Chemistry, Faculty of Science, Kaduna State University, Kaduna, Nigeria.

Email: ugbefabianaudu@gmail.com

### ABSTRACT

This study was aimed at characterizing samples of natural and synthetic goethite ( $\alpha$ -FeOOH) in order to establish their composition and properties. The natural goethite (NGT) sample was obtained from Itakpe area in North Central, Nigeria while the synthetic goethite (SGT) fine particles were synthesized by the air oxidation method. Techniques employed in the investigation included determination of point of zero charge ( $\text{pH}_{\text{pzc}}$ ), Fourier Transform Infrared Spectroscopy (FTIR), X-Ray Fluorescence (XRF), Scanning Electron Microscopy (SEM), Brauner-Emmet-Teller Isotherm (BET) and particle nano-sizer. Results of the study showed that  $\text{pH}_{\text{pzc}}$  of the NGT and SGT were 7.0 and 8.0 respectively. The main surface functional group from FTIR in both samples was the OH while the XRF studies indicated a high content of iron (66.193 % in NGT and 66.4009% in SGT). The SEM analysis revealed a high porosity being associated with SGT than the natural sample. Furthermore, The surface area of SGT as obtained from BET analysis was 797.662  $\text{m}^2/\text{g}$  while the nano-sizer also revealed a near nano-size for the synthesized goethite with particle size of about 172-173 nm. In view of the results of this study, SGT could relatively be used as a more effective adsorbent. It is also believed that both samples will find applications in lots of other analytical processes.

**Keywords:** Adsorption, BET, Natural goethite, Particle nano-sizer, Synthetic goethite

### INTRODUCTION

Iron ore is the most abundant rock forming mineral and composes about 5% of the Earth's Crust (Joan *et al.*, 2015). The most importantly used iron-bearing minerals are the various oxides and oxyhydroxides of iron of which about sixteen are known (Mohammed *et al.*, 2011). Notable ones are; wüstite (FeO), magnetite ( $\text{Fe}_3\text{O}_4$ ), hematite ( $\text{Fe}_2\text{O}_3$ ), iron(II) hydroxide ( $\text{Fe}(\text{OH})_2$ ), bernalite ( $\text{Fe}(\text{OH})_3$ ), goethite ( $\alpha$ -FeOOH), akaganéite ( $\beta$ -FeOOH), lepidocrocite ( $\gamma$ -FeOOH), feroxyhyte ( $\delta$ -FeOOH) and ferrihydrite ( $\text{Fe}_5\text{HO}_8 \cdot 4\text{H}_2\text{O}$  approx.), or  $5\text{Fe}_2\text{O}_3 \cdot 9\text{H}_2\text{O}$  (Mohammed *et al.*, 2011). The most abundant being goethite, hematite and magnetite, followed by ferrihydrite, maghemite and lepidocrocite, but goethite and hematite are by far the most common Fe-oxides in soils. This is partly due to their high thermodynamic stability (Villacís-García *et al.*, 2015; Abdus-Salam and Adekola, 2005; Abdus-Salam and Ikudayisi, 2017).

Goethite ( $\alpha$ -FeOOH), named after Johann Wolfgang von Goethe (1749-1832) is usually a common component of some soils and sediments. The goethite mineral is formed as a result of oxidative weathering and soil formation. Goethite, as other magnetic minerals, such as hematite and maghemite, occurs widely in many soils type (Marcos *et al.*, 2006).

Iron ore deposits have been found in various locations in Nigeria, but mainly in the North-central, North-east and South-east regions. Iron ore deposits in Nigeria typically occur in the following forms: hematite, magnetite, metasedimentary, bands of ferruginous quartzites, sedimentary ores, limonite, maghemite, goethite and siderite (Nigerian Mining Sector, 2012). Some iron ore deposit areas in central Nigeria and their estimated reserves are shown in Table 1.1.

**Table 1.1: Notable Iron Ore Deposits in Central Nigeria**

S/N	Deposit Area	Estimated Reserves (million tonnes)
1	Itakpe	310
2	Ajabanoko	60
3	Agbado-okudu	60
4	Tajimi	20
5	Anomaly K-3	30
6	Anomaly K-2	20
7	Ochokochoko	12
8	Agbaja	370.5

Adapted from: Nigerian Mining Sector (2012)

An investigation carried out by Adedeji and Sale (1984), showed that, Itakpe ore (64%) is richer in iron than the Agbaja ore (54%). Clearly, Itakpe ore is a fairly high-grade, acidic (or siliceous) ore, whereas Agbaja is a low-grade, high-phosphorus and acidic ore.

In literature, iron oxides and oxyhydroxides have been synthesized using several techniques which are generally classified as physical, chemical and biological methods. Commonly used chemical methods include chemical precipitation, sol-gel, flow injection, thermal decomposition, thermal plasma arc method, hydrothermal and solvothermal syntheses, microemulsion, and mono chemical processing. Others are ultrasound irradiation, reverse micelles, hydrolysis and thermolysis of precursors, electro-spray synthesis, and colloidal chemistry method (Mufti *et al.*, 2014; Wu *et al.*, 2015; Tharani and Nheru, 2015; Raiza and Meera, 2016). The major challenges of the chemical methods include low dispersion in solvents, wide particle size distribution, aggregation of particles and the poor uniformity of the size of the particles (Raiza and Meera, 2016). However, co-precipitation, a chemical method, remains one of the commonest techniques for the synthesis of inorganic compounds which is based on the deposition of substances when the saturation point is exceeded.

Characterizing a mineral ore is a necessary step to perform before any processing takes place whereby grade or quality, densities, shape, chemical compositions and physical characteristics are determined to allow for appropriate application of technical parameters (Joan *et al.*, 2015). Common instrumental methods of analysis used in the characterization of goethite and other iron dominated mineral ores include Fourier Transform Infrared Spectroscopy (FTIR) for surface functional groups (Tharani and Nheru, 2015), X-Ray Fluorescence (XRF) or Energy Dispersive X-ray Spectroscopy (EDX) for elemental compositions (Cheng *et al.*, 2012), and Scanning Electron Microscopy (SEM) for grain size and morphological properties (Mufti *et al.*, 2014). Others include X-Ray Diffraction (XRD) for

crystallization phase analysis (Joan *et al.*, 2015), thermal analysis (Gasser *et al.*, 1996), Brauner-Emmet-Teller Isotherm (BET) for surface area determination (Villacis-Garcia *et al.*, 2015), Transmission Electron Microscopy (TEM) (Villacis-Garcia *et al.*, 2015), and particle nano-sizing for particle sizes and size composition (Abdus-Salam and Ikudayisi, 2017).

These various oxides and hydroxides are tremendously diverse in applications such as their use as important ore of iron, as pigment or pigment formulation, use in thermite, and as important adsorbents in the adsorption of anions (Mohammed *et al.*, 2011). Many iron oxides have attracted much attention by their utility as adsorbents and their abundance in nature. Goethite particles display high specific surface areas and strong affinities for surface binding of oxyanions and heavy metals (Villacis-Garcia *et al.*, 2015; Abdus-Salam and Ikudayisi, 2017). Goethite has been used as a model adsorbent because of its well-defined crystal structure since it can be synthesized readily in the laboratory. Many researchers have previously used goethite to adsorb simple inorganic anions, oxyanions and organic ions. These include Lead (II) and zinc (II) (Abdus-Salam and Adekola, 2005), As (III) and As (V) (Giménez *et al.*, 2007), phosphate and arsenate (Gao and Mucci, 2003), and cadmium ion (Salami and Adekola, 2002). Amongst others are copper and zinc ions (Gunton *et al.*, 2005), Arsenic oxyanions (Matis *et al.*, 1997), soil humic acid (Antelo *et al.*, 2007), fulvic acid (Filius *et al.*, 2007), selenium (IV) and (VI) (Balistrieri and Chao, 1987), and methylene blue (Nassar and Ringsred, 2012).

The primary objective of this research was to obtain goethite from its natural deposit, synthesize goethite, and characterize them using FTIR, XRF, SEM, BET, and nano-sizing analytical techniques in order to establish their composition and properties, and to provide insight into their suitability for adsorption and certain practical applications.

## MATERIALS AND METHODS

### Sample Collection

Sample of natural goethite (NGT) of high grade quality was collected from the National Iron Ore Mining Company (NIOMCO), Itakpe in Kogi State, Central Nigeria. 5.0 kg sample was washed, air-dried, ground and screened to pass through a 0.112mm analytical sieve to remove larger particles. The sample was then kept in a sterilized sample bottle for further use (Ugbe *et al.*, 2014).

### Synthesis of Goethite ( $\alpha$ -FeOOH) Particles (GT)

Goethite ( $\alpha$ -FeOOH) particles were synthesized by dissolving 10 g of  $\text{FeCl}_2 \cdot 4\text{H}_2\text{O}$  in 1000 ml of de-ionized water and then 110 ml of 1M  $\text{NaHCO}_3$  was added to the solution at room temperature. After air-oxidation of the resulting solution for approximately 25 minutes, yellow deposits of goethite particles were formed and thereafter, separated from the solution by filtration followed immediately by washing 5 times with ethanol and de-ionized water to remove adhering impurities. The particles were then oven dried at 70 °C for an hour to obtain the synthetic goethite (SGT), which was thereafter kept in a sterilized sample bottle for further use (Lee *et al.*, 2004).

### Determination of Point of Zero Charge

The point of zero charge ( $\text{pH}_{\text{pzc}}$ ) of both goethite samples (NGT and SGT) were measured by using the pH drift method (Abdus-Salam and Adekola, 2005). The pH of 50 ml of 0.1 mol/L KCl solutions was adjusted by using 0.1M HCl or 0.1M NaOH to pH of 2, 3, 4, 5, 6, 7, 8, 9, 10, 11 and 12. 0.05 g of each goethite was then added to the solutions in the reaction bottles separately and left

at room temperature for 24 hrs. After the pH was stabilized, the final pH was then taken with pH meter and recorded. A graph of  $\text{pH}_{\text{initial}}$  versus pH drift ( $\text{pH}_{\text{final}} - \text{pH}_{\text{initial}}$ ) was drawn and used to determine the points at which the initial and the pH drift values are equal. The point of intersection of the curve on the initial pH axis (i.e. when  $\Delta\text{pH}=0$ ) is the point of zero charge for the goethite (Vijayakumar *et al.*, 2012).

### Instrumental Methods of Characterization

Further characterizations were carried out on both samples (NGT and SGT) using the following instrumental methods; XRF, FTIR (SHIMADZU Series), SEM, BET (Nova Station C BET instrument), and particle nano-sizer (Malvern instrument). The combination of these analyses provided information on the percentage composition, the crystal structure, defect structure, chemical composition, particle size and size composition (Hayle *et al.*, 2014; SharmilaDevi *et al.*, 2014; Parthasarathi and Thilagavathi, 2009).

## RESULTS AND DISCUSSION

### Point of Zero Charge

The  $\text{pH}_{\text{pzc}}$  of NGT and SGT which is the pH at which the net charge on the surface of the goethite is zero, was determined by the pH drift method and the results were plotted for both samples (Figures 1.1a and b respectively). It was observed that, the  $\text{pH}_{\text{pzc}}$  of SGT and NGT samples were 8.0 and 7.0 respectively, depicting that the surface of both samples were positive at pH lower than  $\text{pH}_{\text{pzc}}$  and negative at pH higher than the  $\text{pH}_{\text{pzc}}$ . This trend was also reported by Abdus-Salam and Adekola (2005).

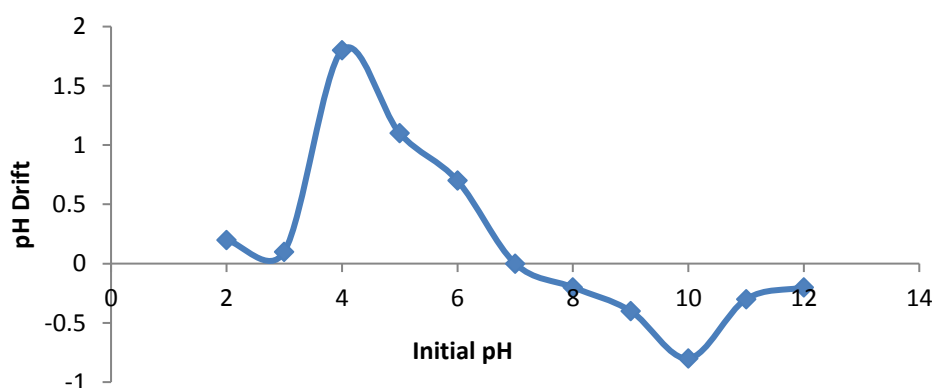


**Figure 1.1a: Point of zero charge curve for NGT**

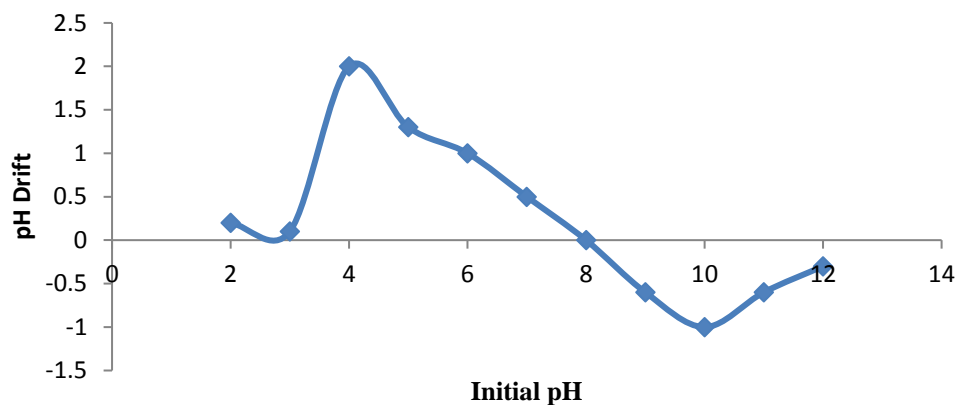


**Figure 1.1b: Point of zero charge curve for SGT.**

#### Fourier Transforms Infrared Spectroscopy

FTIR is a technique for analyzing the functional groups on the surface of the goethite. The FTIR spectra can be shown for NGT and SGT (Figures 1.2a and b respectively). The spectra of the natural and synthetic goethite samples were recorded over the range of 4000 – 500  $\text{cm}^{-1}$ . A weak and medium peak was observed around 3454.62  $\text{cm}^{-1}$  for NGT while the SGT particles showed a strong and broad peak at 3421.83  $\text{cm}^{-1}$  which were attributed to the presence of O-H (bond) stretching vibrations. A weak and less prominent peak at 1616.40  $\text{cm}^{-1}$  for NGT, and a medium and sharp peak observed at 1627  $\text{cm}^{-1}$  for

SGT were attributed to H-O-H bending vibrations. A sharp and strong peak observed around 1080.17 and a weak peak at 1170.83  $\text{cm}^{-1}$  were due to the presence of Fe-OH hydroxo complexes (Adegoke *et al.*, 2013). The peaks observed at 524.66  $\text{cm}^{-1}$  and 451.00  $\text{cm}^{-1}$  for NGT, and 559  $\text{cm}^{-1}$  and 418.57  $\text{cm}^{-1}$  for SGT were assigned to the Fe-O bond stretching and bending vibrations respectively (Adegoke *et al.*, 2013). Therefore, it can be concluded that the strong, sharp and more prominent peaks associated with SGT particles showed it contains goethite in its pure form than the NGT sample.

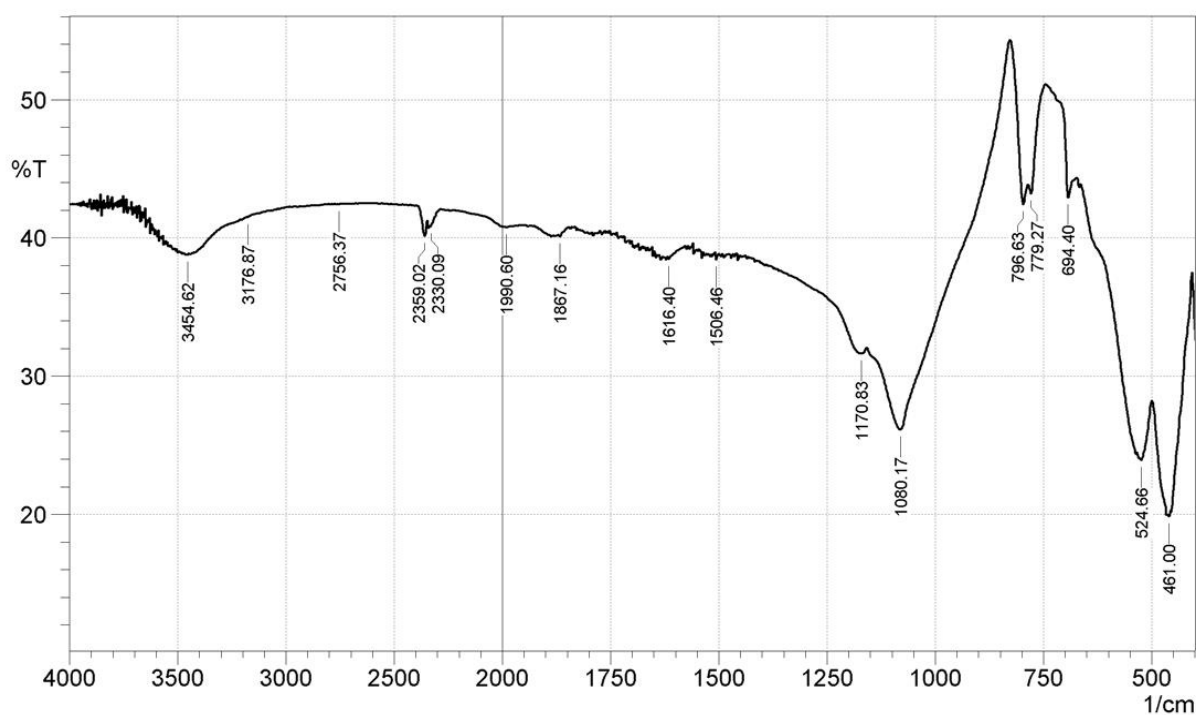


**Figure 1.2a: IR spectrum of NGT**

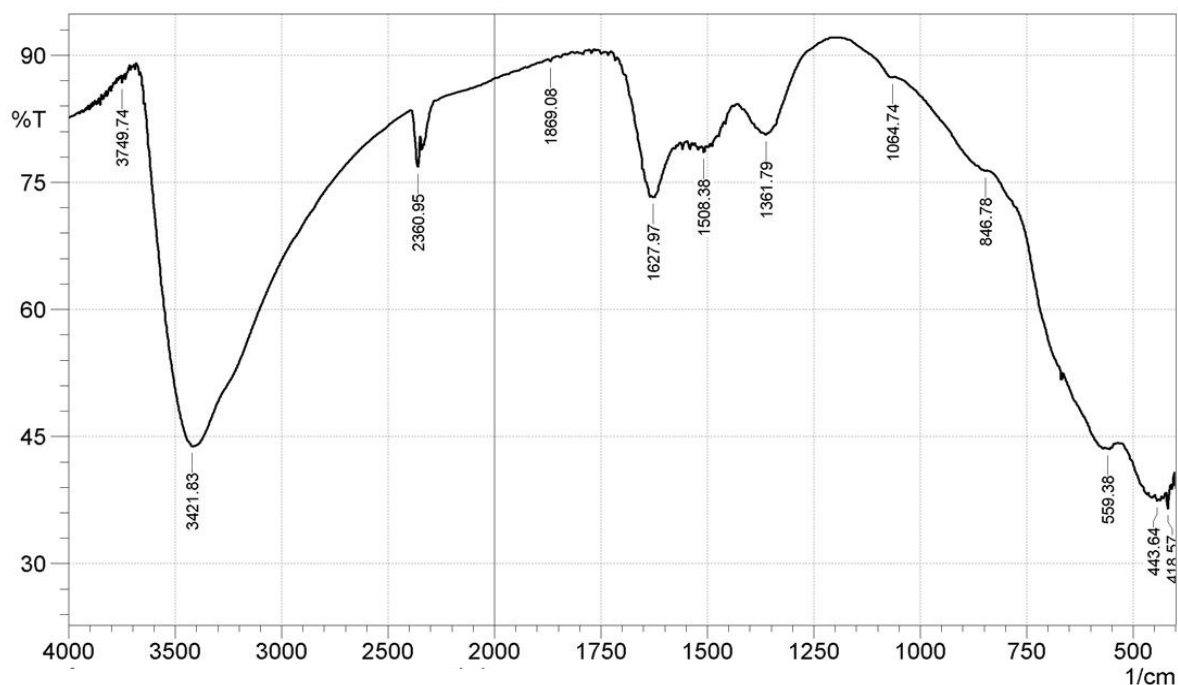


**Figure 1.2b: IR spectrum of SGT**

### X-ray Fluorescence

The elemental composition of each sample was determined by the XRF technique. The results obtained from the analysis were presented in Table 1.2. It was observed as expected that the major element present in both goethite samples (NGT and SGT) was iron with composition by mass of 66.193 % in NGT and 66.4009% in SGT. Other elements

were present as trace or ultra trace. The percentage composition by mass of iron in both samples can be compared to that obtained from the goethite mineral data (62.85% Fe in goethite). The relatively higher percentage composition by mass of SGT may be due to a higher degree of purity associated with it than NGT.

**Table 1.2: The elemental composition of NGT and SGT samples**

NGT		SGT	
Element	Content (%)	Element	Content (%)
P	0.0151	Mg	0.0182
Ca	0.1346	P	0.0032
V	0.0204	Ca	0.0902
Cr	0.0556	V	0.0210
Mn	0.0946	Cr	0.0619
Co	0.4262	Mn	0.0823
Fe	66.1930	Co	0.4024
Ni	0.0572	Fe	66.4009
Cu	0.0205	Ni	0.0724
Zn	0.0320	Cu	0.0196
Pb	0.1927	Zn	0.0361
Sn	0.1238	Pb	0.2151
Sb	0.0764	Rb	0.0077
Rb	0.0066	Mo	0.0849
		Sn	0.1202
		Sb	0.0672

### Scanning Electron Microscopy

SEM is a technique used to determine the shape, texture and morphology of a sample (Abdus-Salam and Itiola, 2012). The micrographs obtained for NGT and SGT were presented in Figures 1.3a and b respectively. The SEM micrograph of the natural goethite (Figure 1.3a) showed the exhibition of different morphological shapes such as plate-like, needle-like and hexagonal (Adegoke *et al.*, 2013). The textures, shapes and sizes of the particles in the natural goethite showed heterogeneous nature of the natural sample, which confirms that many other compounds were present in the sample. Additionally, a good level of porosity was observed

in the micrograph of the natural goethite sample which serves as sites for binding with other materials.

On the other hand, the SEM micrograph of the SGT particles (Figure 1.3b) showed dense iron oxide which was found to exhibit irregular shape and tends to agglomerate. The SGT particles were smaller, homogenous and far from one another thereby creating pores within the structure of the goethite. Furthermore, surface of the SGT particles exhibited large pores, an indication of high porosity as also observed by Lee *et al.* (2004). The observed porosity on the surface of both goethite accounts for their good practical applicability in adsorption processes.

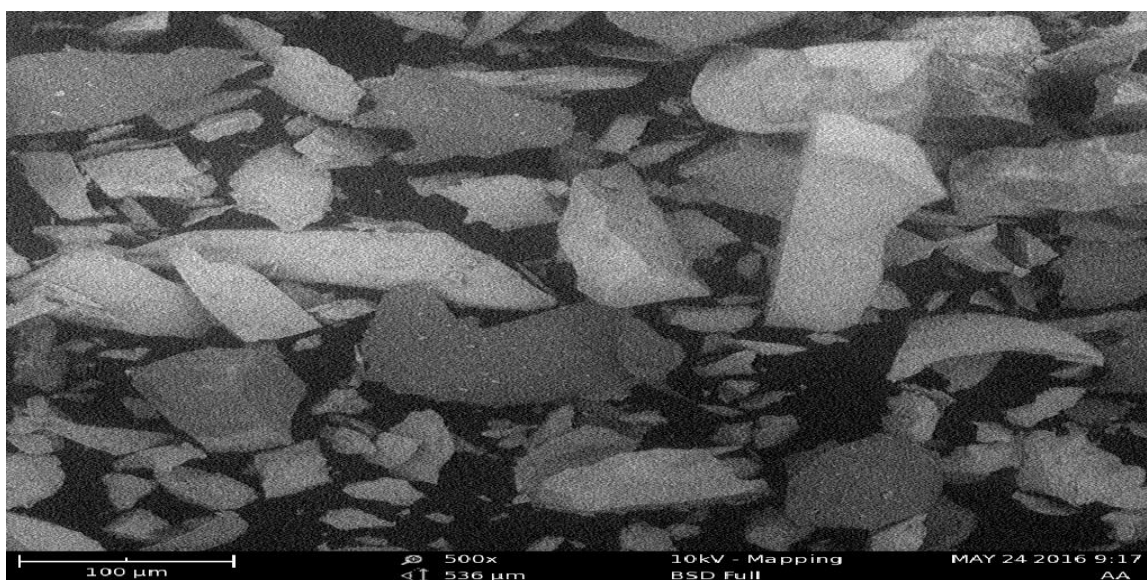


Figure 1.3a: SEM micrograph of NGT (Mag X 500x)

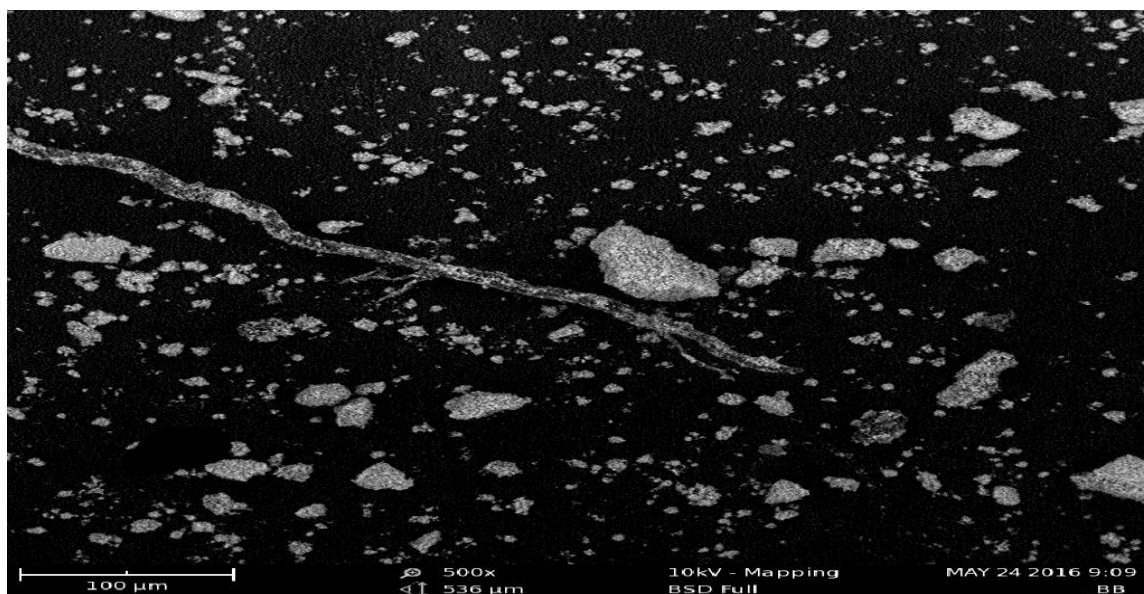


Figure 1.3b: SEM micrograph of SGT (Mag X 500x)

**Specific surface area determination**

The specific surface area (SSA) of SGT was determined by the BET method on Nova Station C BET instrument and nitrogen was used as the adsorbate (Table 1.3). Experimental BET results showed that SGT has a multipoint surface area of 797.66 m<sup>2</sup>/g. According to Villalobos and

Perez-Gallegos (2008), an ‘ideal crystal’ of goethite is that in which its SSA is greater than 80 m<sup>2</sup>/g. Therefore, SGT fall into this category, indicating why many researchers report goethite as having excellent applicability in adsorption processes.

**Table 1.3: Summary of BET data for SGT**

Surface Area Data	
Singlepoint BET.....	6.080e+02 m <sup>2</sup> /g
Multipoint BET.....	7.977e+02 m <sup>2</sup> /g
Langmuir surface area.....	1.894e+03 m <sup>2</sup> /g
t-method external surface area.....	7.977e+02 m <sup>2</sup> /g
DR method micropore area.....	1.011e+03 m <sup>2</sup> /g
DFT cumulative surface area.....	2.565e+02 m <sup>2</sup> /g

**Particle nano-sizing Technique**

Malvern particle nano-sizer was used to determine the size of the particle of the synthesized goethite. The size composition of the goethite was also revealed by the volume and intensity using this method as shown in Figures 1.4a-b. It was observed that the synthesized goethite is heterogeneous in size, but the most prominent of the sizes fall within 172 – 173 nm which is near nano-size particles defined as materials with sizes within the range of 1 – 100nm, “although there are examples of nanoparticles several hundreds of

nanometer in size made of inorganic and organic materials, which have many novel properties compared with bulk materials” (Tharani and Nheru, 2015). This observation has been illustrated by both the percentage intensity and the percentage volume of 43.7% and 38.5% respectively. The results also showed that the synthesized goethite contained aggregates and it fluoresce upon exposure to electromagnetic radiation. It can be concluded therefore that the synthetic goethite is just fine particles with sizes near that of a nano-material.

**Results**

<b>Z-Average (d.nm):</b> 1149	<b>Peak 1:</b> 172.3	<b>Size (d.nm):</b> 172.3	<b>% Intensity:</b> 43.7	<b>St Dev (d.nm):</b> 21.66
<b>Pdl:</b> 0.944	<b>Peak 2:</b> 122.9	<b>Size (d.nm):</b> 122.9	<b>% Intensity:</b> 31.0	<b>St Dev (d.nm):</b> 13.59
<b>Intercept:</b> 0.493	<b>Peak 3:</b> 757.1	<b>Size (d.nm):</b> 757.1	<b>% Intensity:</b> 22.9	<b>St Dev (d.nm):</b> 162.0
<b>Result quality Refer to quality report</b>				

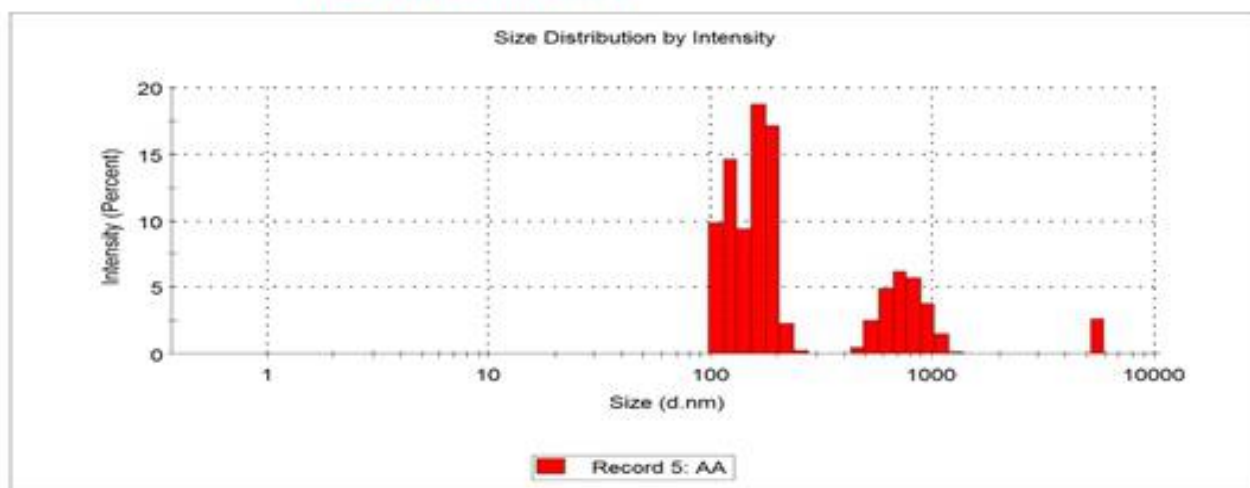


**Figure 1.4a: The size distribution of SGT by intensity**

## Results

	Size (d.n...	% Volume:	St Dev (d.n...
<b>Z-Average (d.nm):</b> 1149	<b>Peak 1:</b> 173.6	38.5	26.59
<b>Pdl:</b> 0.944	<b>Peak 2:</b> 121.4	31.3	16.60
<b>Intercept:</b> 0.493	<b>Peak 3:</b> 842.1	22.5	191.9
<b>Result quality Refer to quality report</b>			

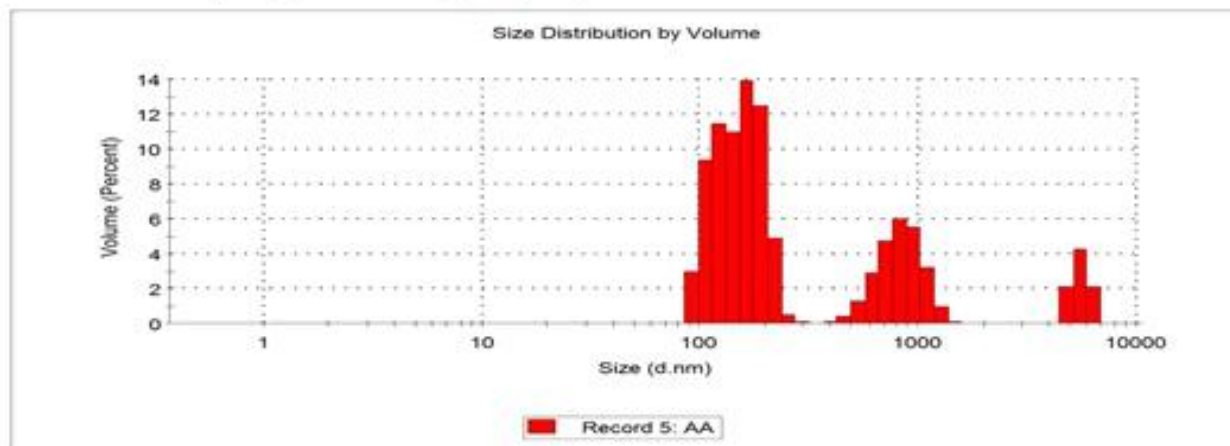


**Figure 1.4b: The size distribution of SGT by volume**

## CONCLUSION

In this study, a natural goethite and synthesized goethite samples were characterized. Based on the results of the study, the  $pH_{pzc}$  of the NGT and SGT were 7.0 and 8.0 respectively. The major functional group on both samples was OH as revealed by the results of FTIR analysis. The SEM analysis showed a high porosity and more regular shapes of particles being observed with SGT than NGT. The main elemental composition of both goethite forms was iron with percentage composition by mass of 66.1930% and 66.4009% for NGT and SGT respectively as obtained via XRF analysis. Additionally, the BET surface area determined showed high value of  $797.662\text{m}^2/\text{g}$ , whilst the size of SGT particles predominantly fall within 172 – 173 nm which are near nano-scale. Therefore, the combined result of the characterization showed that SGT could be used as a more effective adsorbent than NGT. It is equally believed that the various technical investigations carried out on both samples will help them (NGT and SGT) to find applications in several other analytical procedures.

## REFERENCES

- Abdus-Salam, N. and Adekola, F.A. (2005) Physico-chemical characterization of some Nigerian goethite mineral samples. *Ife J. Sci.*, 7(1), 131-137.
- Abdus-Salam, N. and Ikudayisi, V.A. (2017). Preparation and characterization of synthesized goethite and goethite-date palm seeds charcoal composite. *Ife J. Sci.*, 19(1), 99-107.
- Abdus-Salam, N. and Itiola, A.D. (2012) Potential application of termite mound for adsorption and removal of Pb (II) from aqueous solutions. *J. Iranian Chem. Soc.*, 9, 373-382.
- Adedeji, F.A. and Sale, F.R. (1984). Characterization and reducibility of Itakpe and Agbaja (Nigerian) iron ores. *Clay Minerals*, 19(5), 843-856.
- Adegoke, H.I., Adekola, F.A., Fatoki, O.S. and Ximba, B.J. (2013). Adsorption of Cr (VI) on synthetic hematite ( $\alpha\text{-Fe}_2\text{O}_3$ ) nanoparticles of different morphologies. *Korean J. Chem. Eng.*, 31(1), 142-154.
- Antelo, J., Arce, F., Avena, M., Fiol, S., López, R. and Macías, F. (2007). Adsorption of a soil humic acid at the surface of goethite and its competitive interaction with phosphate. *Geoderma*, 138(1-2), 12-19.
- Balistreri, L.S. and Chao, T.T. (1987). Selenium adsorption by goethite. *Soil Sci. Soc. American J.*, 51(5), 1145-1151.
- Cheng, Z., Tan, A.K., Tao, Y., Shan, D., Ting, K.E. and Yin, X.J. (2012). Synthesis and characterization of iron oxide nanoparticles and applications in the removal of heavy metals from industrial wastewater. *Int. J. Photo-energy*, doi:10.1155/2012/608298.
- Filius, J.D., Lumsdon, D.G., Meeussen, C.L., Hiemstra, T. and Van Riemsdijk, W.H. (2007). Adsorption of fulvic acid on goethite. *Geochimica et Cosmochimica Acta.*, 64(1), 51-60.

- Gao, Y. and Mucci, A. (2003). Individual and competitive adsorption of phosphate and arsenate on goethite in artificial seawater. *Chem. Geo.*, 199, 91– 109.
- Gasser, U.G., Jeanroy, E., Mustin, C., Barres, O., Nuesch, R., Berthelin, J. and Herbillon, A.J. (1996) Properties of synthetic goethites with Co for Fe substitution. *Clay Minerals*, 31, 465-476.
- Gim'enez, J., Mart'inez, M., Pablo, J., Rovira, M. and Duroc, L. (2007). Arsenic sorption onto natural hematite, magnetite, and goethite. *J. Hazard Mat.*, 141, 575–580.
- Goethite minerals data (n.d.). Accessed on 14/09/2016 from <https://webminerals.com>.
- Gunton, C., Christy, A.G. and McPhail, D.C. (2005). The effect of anions on the adsorption of copper and zinc onto goethite. *Regolith – Ten Years of CRC LEME*, 125-128.
- Hayle, S., Talbachew, G. and Gonfa, G. (2014). Synthesis and characterization of titanium oxide nanomaterials using sol-gel method. *American J. Nanosci. Nanotech.*, 2(1), 1-7.
- Joan, J.K., Alex, M.M., Augustine, B.M. and Stephen, K.K. (2015). Characterization of selected mineral ores in the Eastern Zone of Kenya: Case study of Mwingi North Constituency in Kitui County. *Int. J. Mining Eng. Mineral Proc.*, 4(1), 8-17.
- Lee, G.H., Kim, S.H., Choi, B.J. and Huh, S.H. (2004). Magnetic properties of needle-like  $\alpha$ -FeOOH and  $\gamma$ -FeOOH nanoparticles. *J. Korean Phy. Soc.*, 45(4), 1019-1024.
- Marcos, A.E., Chaparro, A., Ana, M.S., Juan, C.B. and Raúl, E. (2006). Magnetic studies of natural goethite samples from Tharsis, Huelva, Spain. *Geofísica Int.*, 45(4), 219-230.
- Matis, K.A., Zouboulis, A.I., Malamas, F.B., Afonso, M.D. and Hudson, M.J. (1997). Flotation removal of As (V) onto goethite. *Environ. Poll.*, 97 (3), 239-245.
- Mohammed, M.R., Sher, B.K., Aslam, J., Mohd, F. and Abdullah, M.A. (2011). Iron oxide nanoparticles, nanomaterials, Prof. Mohammed Rahman (Ed.), ISBN: 978-953-307-913-4, In Tech, Available from: <http://www.intechopen.com/books/nanomaterials/iron-oxide-nanoparticles>, accessed on 13/05/2016.
- Mufti, N., Atma, T., Fuad, A. and Sutadji, E. (2014) Synthesis and characterization of black, red and yellow nanoparticles pigments from the iron sand. *AIP Conf. Proc.*, 1617, 165-169.
- Nassar, N.N. and Ringsred, A. (2012). Rapid adsorption of methylene blue from aqueous solutions by goethite nano-adsorbents. *Environ. Eng. Sci.*, 29(8), 790-797.
- Nigerian Mining Sector (2012) Brief. <https://home.kpmg.com/content/dam/kpmg/ng/pdf/advisory/ng-Nigerian-Mining-Sector.pdf>, p9, accessed 24 Jan 2018.
- Parthasarathi, V. and Thilagavathi, G. (2009). Synthesis and characterization of titanium dioxide nanoparticles and their applications to textiles for microbe resistance. *J. textile Apparel Tech Mgt.*, 6(2), 1-8.
- Raiza, R. and Meera, V. (2016). Synthesis of iron oxide nanoparticles coated sand by biological method and chemical method. *Proc. Tech.*, 24, 210 – 216.
- Salami, N. and Adekola, F.A. (2002). A Study of Sorption of Cadmium by Goethite in Aqueous Solution. *Bulletin Chem. Soc. Ethiopia*, 16, 1, 1-7.
- SharmilaDevi, R., Venkatesh, R. and Rajeshwari, S. (2014). Synthesis of titanium dioxide nanoparticles by sol-gel technique. *Int. J. Innovative Res. Sci., Eng. Tech.*, 3 (8), 15206- 15211.
- Tharani, K. and Nehru, L.C. (2015). Synthesis and characterization of iron oxide nanoparticle by precipitation method. *Int. J. Adv. Res. Phy. Sci.*, 2(8), 47-50.
- Ugbe, F.A., Pam, A.A. and Ikudayisi, V.A. (2014). Thermodynamic study of chromium (III) ion adsorption by sweet orange (*citrus sinensis*) peels adsorbent. *American J. Analytical Chem.*, 5, 666-673.
- Vijayakumar, G., Tamilarasan, R. and Dharmendirakumar, M. (2012). Adsorption, kinetic, equilibrium and thermodynamic studies on the removal of basic dye rhodamine-B from aqueous solution by the use of natural adsorbent perlite. *J. Mat. Environ. Sci.*, 3 (1), 157-170.
- Villacís-García, M., Ugalde-Arzate, M., Vaca-Escobar, K. and Villalobos, M. (2015). Laboratory synthesis of goethite and ferrihydrite of controlled particle sizes. *Boletín de la Sociedad Geológica Mexicana*, 67(3), 433-446.
- Villalobos, M. and Perez-Gallegos, A. (2008). Goethite surface reactivity: A macroscopic investigation unifying proton, chromate, carbonate, and lead (II) adsorption. *J. Colloid and Interface Sci.*, 326, 307-323.
- Wu, W., Wu, Z., Yu, T., Jiang, C. and Kim, W. (2015). Recent progress on magnetic iron oxide nanoparticles: synthesis, surface functional strategies and biomedical applications. *Sci. Tech. Adv. Mater.*, 16, 1-43.